

## Segregation trends of the metal alloys Mo–Re and Mo–Pt on Hf O 2 : A first-principles study

A. A. Knizhnik, A. V. Gavrikov, A. A. Safonov, I. M. Iskandarova, A. A. Bagatur'yants, B. V. Potapkin, L. R. C. Fonseca, and M. W. Stoker

Citation: *Journal of Applied Physics* **100**, 013506 (2006); doi: 10.1063/1.2209768

View online: <http://dx.doi.org/10.1063/1.2209768>

View Table of Contents: <http://scitation.aip.org/content/aip/journal/jap/100/1?ver=pdfcov>

Published by the [AIP Publishing](#)

---

### Articles you may be interested in

[Electrical transport and magnetic properties of superconducting Mo 52 Re 48 alloy](#)  
*AIP Conf. Proc.* **1512**, 1092 (2013); 10.1063/1.4791426

[Segregation of tungsten at \( L 1 2 \) / \( fcc \) interfaces in a Ni-based superalloy: An atom-probe tomographic and first-principles study](#)  
*Appl. Phys. Lett.* **93**, 201905 (2008); 10.1063/1.3026745

[The study of surface segregation of Re 3 Pt polycrystalline alloy with photoelectron spectroscopy](#)  
*J. Chem. Phys.* **129**, 174707 (2008); 10.1063/1.2987704

[Combinatorial study of Ni–Ti–Pt ternary metal gate electrodes on Hf O 2 for the advanced gate stack](#)  
*Appl. Phys. Lett.* **89**, 142108 (2006); 10.1063/1.2357011

[Electronic topological transition in Re 1x Mo x alloys and its influence on the temperature of the superconducting transition](#)  
*Low Temp. Phys.* **30**, 388 (2004); 10.1063/1.1739133

---



**AIP** | Journal of Applied Physics

*Journal of Applied Physics* is pleased to announce **André Anders** as its new Editor-in-Chief

## Segregation trends of the metal alloys Mo–Re and Mo–Pt on HfO<sub>2</sub>: A first-principles study

A. A. Knizhnik,<sup>a)</sup> A. V. Gavrikov, A. A. Safonov, I. M. Iskandarova, A. A. Bagatur'yants, and B. V. Potapkin

*Kinetic Technologies Ltd., Kurchatov Square, 1, Moscow, 123182, Russia*

L. R. C. Fonseca<sup>b)</sup>

*Center for Semiconductor Components, Universidade Estadual de Campinas, Caixa Postal 6061, Campinas, São Paulo 13083-870, Brazil*

M. W. Stoker

*Freescale Semiconductor, Inc., 2100 E. Elliott, Tempe, Arizona 85284*

(Received 17 January 2006; accepted 21 April 2006; published online 7 July 2006)

Using first-principles calculations, we compared the segregation trends at the surface of metal alloys with those at an interface with HfO<sub>2</sub>. The choice of this oxide was motivated by its significance as a potential replacement for SiO<sub>2</sub> in advanced transistors. We considered Mo–Re and Mo–Pt alloys as typical examples of disordered and ordered alloys, respectively. The segregation to the surface/interface was analyzed in terms of metal and oxygen adsorption energies. It is shown that chemical bonding at the metal/oxide interface strongly influences segregation both in Mo–Re and Mo–Pt alloys. In particular, bonding with oxygen atoms at the oxide/Mo–Re alloy interface depletes the Re content of the interfacial layer. In the case of Mo–Pt on HfO<sub>2</sub> an oxygen-rich interface promotes the formation of one monolayer (but not two monolayers) of Mo separating PtMo<sub>x</sub> from HfO<sub>2</sub>, while a stoichiometric interface favors an abrupt PtMo<sub>x</sub>/HfO<sub>2</sub> interface. This study also shows that the presence of Mo in the alloy stabilizes Pt which can potentially decrease the tendency of Pt to diffuse into the oxide matrix. The individual constituents of these intermetallic compounds exhibit high vacuum work functions, and therefore these alloys are also likely to have sufficiently high work functions to be considered as promising candidates for *p*-type gate electrodes in future generations of transistors. © 2006 American Institute of Physics. [DOI: 10.1063/1.2209768]

### I. INTRODUCTION

Metal alloys in thin films have attracted considerable attention in various fields of science and technology, such as microelectronics, catalysis, and coatings. The surface composition of alloys usually differs from that of the bulk material as a result of species migration driven by surface rearrangement and energy minimization. Segregation has been the subject of numerous experimental and theoretical studies.<sup>1–4</sup> In general the segregation trends of chemically ordered alloys, where the different chemical species exclusively occupy sublattices of the crystal lattice, differ from those of disordered alloys.<sup>2,3</sup> Chemical ordering occurs in systems with a large negative enthalpy of mixing, whereas systems with little or no enthalpy of mixing usually form disordered alloys. As a consequence, the enthalpy of mixing plays a significant role in determining the segregation of ordered alloys, while surface energy is the dominant factor controlling segregation of disordered alloys.

It has been mentioned in the literature that segregation can be affected by chemisorption of atoms/molecules on the surface of metal alloys,<sup>3,5–7</sup> since the interaction of the various alloy components with a given adsorbate will not in general be the same. Similar effects are expected at the in-

terface of a metal alloy with another material, due to differences in the chemical bonding of metal atoms at this interface. In this work we theoretically consider segregation in two metal alloys (ordered Mo–Pt and disordered Mo–Re) forming a metal/*m*-HfO<sub>2</sub> interface and compare it with the surface segregation of the pure alloys. Hafnia was selected as the substrate material due to its potential application as a high dielectric constant (high-*k*) replacement for SiO<sub>2</sub> in advanced microelectronic devices. The continuation of the current downscaling of transistor dimensions will soon lead to severe problems of leakage through SiO<sub>2</sub>, increasing power consumption to unacceptable levels. A high-*k* dielectric can, in principle, allow for the use of a thicker oxide, thus avoiding excessive leakage, while maintaining a sufficiently large capacitance to provide the desired electrical device characteristics.<sup>8</sup> In addition the gate electrode, currently polysilicon (poly-Si) is expected to be replaced by metal gates to avoid the degradation of the high-*k* material observed during poly-Si deposition and to eliminate poly-Si depletion which leads to a loss of capacitance.<sup>9</sup> Suitable metal gates must have effective work functions (WFs) close to the valence band edge [for *p*-type metal-oxide semiconductor (PMOS) devices] or the conduction band edge [for *n*-type metal-oxide semiconductor (NMOS) devices] of the Si substrate<sup>10</sup> in bulk complementary metal-oxide semiconductor (CMOS). Metal alloys are potentially more stable as metal gates than pure metals. Moreover, Mo–Pt and Mo–Re

<sup>a)</sup>Electronic mail: knizhnik@kintech.ru

<sup>b)</sup>Electronic mail: fonsecalcrc@yahoo.com

alloys are made of high WF components and thus may also display a high WF while being more stable at the interface with HfO<sub>2</sub> than their individual components. However, the band alignment across the metal/oxide interface is very sensitive to the interface stoichiometry.<sup>9,11</sup> Therefore a good understanding of the segregation process for these alloys on HfO<sub>2</sub> may bring important information about general trends for segregation in the presence of interfaces and about the feasibility of these two and other similar alloys as metal gates in advanced transistors.

Mo–Re is a typical example of a random alloy, whose segregation properties have been studied in a number of experimental works.<sup>12–15</sup> The available literature data show that in the Mo–Re system, homogeneous solid solutions with bcc structures can be formed at low temperatures for Re contents below 25–30 at. %.<sup>16,17</sup> They also show significant Mo segregation in Mo–Re alloys for the bcc(100) surface with an oscillating concentration profile that decays from the surface to the bulk, while segregation on bcc(110) is less pronounced at high temperatures, of the order of 2000 K.<sup>15</sup> Ouannasser and Dreyse<sup>18</sup> computed the surface compositions of a Mo<sub>0.75</sub>Re<sub>0.25</sub>(100) random alloy using the tight-binding (TB) recursion method and found very strong Mo enrichment in the surface plane. More recently, Deng *et al.*<sup>19</sup> applied a kinetic Monte Carlo model based on empirical potentials to study segregation in Mo–Re alloys as a function of the surface orientation and alloy composition.

Mo–Pt is a typical example of an ordered alloy as it can crystallize in several intermediate phases. The alloy composition Pt<sub>2</sub>Mo is one such phase which can be obtained under certain conditions.<sup>20,21</sup> Experimental data on the segregation of Mo–Pt show that the intermediate Pt<sub>2</sub>Mo phase is formed when a thin layer of Mo is deposited on the Pt(111) surface and the system is annealed at ~700 K.<sup>22,23</sup> One should note that without the formation of such an intermediate alloy, Pt segregation to the surface would be expected based on theoretical segregation energy data<sup>4</sup> since Pt has a smaller surface energy than Mo.

While previous studies have investigated segregation trends in pure Mo–Re and Mo–Pt alloys, the segregation of these alloys when forming an interface with an oxide has not been considered before and it is unclear how such an interface may affect segregation. The goal of this study is to understand the driving forces behind the interface segregation of Mo–Re and Mo–Pt supported on the *m*-HfO<sub>2</sub>(001) surface.

The paper is organized as follows: In Sec. II we describe the computational methods used in this study and the atomic structure of the simulated metal/*m*-HfO<sub>2</sub> interfaces, in Sec. III we analyze the surface properties of the alloys considered in this work, in Sec. IV we analyze the interface properties of those alloys on a HfO<sub>2</sub> substrate, and in Sec. V we present our conclusions.

## II. COMPUTATIONAL DETAILS

The structural and electrical bulk and surface properties of *m*-HfO<sub>2</sub>, of Mo–Re and Mo–Pt alloys, and of Mo–Re/*m*-HfO<sub>2</sub> and Mo–Pt/*m*-HfO<sub>2</sub> interfaces were inves-

tigated using the local density approximation<sup>24</sup> (LDA) of density functional theory<sup>25</sup> (DFT), with core electrons replaced by pseudopotentials (PPs) and valence states described by a plane wave (PW) basis set as implemented in the VASP code.<sup>26</sup> Ultrasoft nonlocal PPs Ref. 27 were used for all the atomic species. Relativistic PPs for Hf, Mo, Re, and Pt were obtained for the neutral atomic configurations 5d<sup>3</sup>6s<sup>1</sup>, 4p<sup>6</sup>5d<sup>5</sup>6s<sup>1</sup>, 5d<sup>6</sup>6s<sup>1</sup>, and 5d<sup>9</sup>6s<sup>1</sup>, respectively. The PW basis was expanded up to a cutoff energy of 495 eV for bulk and surface calculations and 396 eV for interface calculations; sampling of *k* space was achieved using a 5 × 5 × 1 *k*-point Monkhorst-Pack grid for interface calculations. The structures of all slabs were fully optimized until the maximum residual force was less than 0.07 eV/Å.

The calculated bulk lattice constants for bcc Mo (*a* = 3.123 Å), hcp Re (*a* = 2.74 Å and *c* = 4.39 Å), and fcc Pt (*a* = 2.763 Å) are in good agreement with corresponding experimental values of *a* = 3.147 Å, *a* = 2.761 Å and *c* = 4.456 Å, and *a* = 2.775 Å,<sup>28</sup> respectively. The calculated cell vectors of the *m*-HfO<sub>2</sub> phase (*a* = 5.035 Å, *b* = 5.106 Å, *c* = 5.200 Å, and β = 99.52°) are within typical LDA/DFT error from experimental data [*a* = 5.117 Å, *b* = 5.175 Å, *c* = 5.295 Å, and β = 99.18° Ref. 29]. The optimized structure of body-centered orthorhombic Pt<sub>2</sub>Mo has cell vectors *a* = 2.743 Å, *b* = 3.936 Å, and *c* = 8.251 Å. This structure closely resembles the fcc Pt structure: Pt and Mo atoms are 12-fold coordinated with Pt–Pt bond distances of 2.788, 2.743, and 2.706 Å and Pt–Mo bond distances of 2.754, 2.743, and 2.773 Å, all quite close to the Pt–Pt bond length in fcc Pt (2.763 Å from calculation). The (110) surface of the Pt<sub>2</sub>Mo structure corresponds to the (111) surface of fcc Pt. The calculated formation enthalpy of the Pt<sub>2</sub>Mo alloy is –1.15 eV/Pt<sub>2</sub>Mo and indicates the strong thermodynamic stability of this alloy, consistent with phase diagram data.<sup>20</sup>

To investigate segregation at the Mo–Pt/HfO<sub>2</sub> and Mo–Re/HfO<sub>2</sub> interfaces, we employed (2 × √3)Pt(111)/(1 × 1)*m*-HfO<sub>2</sub>(001) and (2 × √3)Mo(110)/(1 × 1)*m*-HfO<sub>2</sub>(001) interface model unit cells, similar to the model used previously to investigate the electrical properties of the Mo(110)/*m*-ZrO<sub>2</sub> interface.<sup>11</sup> The surface supercell sizes were set to experimental *m*-HfO<sub>2</sub> sizes (*a* = 5.117 Å and *b* = 5.175 Å). To conform to the *m*-HfO<sub>2</sub> unit cell vectors, the Pt slab was expanded along the *b* axis by 7.0% and contracted along *a* axis by 6.4% while the Mo slab was expanded along the *b* axis by 4.8% and contracted along the *a* axis by 8.2%. Since the axial deformations have opposite signs (expansion in one direction and contraction in another), their influence on the calculated electronic and thermodynamic properties is small as will be demonstrated below. A Re/*m*-HfO<sub>2</sub> model interface was not considered because as we shall see in Sec. IV it is energetically unfavorable for Re to segregate from the Mo–Re matrix to the Mo–Re/HfO<sub>2</sub> interface.

The interfaces contain six Pt(111) or six Mo(110) layers, four layers of monoclinic (001) HfO<sub>2</sub> (the thickness of the oxide layer is about 10 Å), and a vacuum gap with a thickness of about 10 Å. Two cases were considered: interfaces with a full (four O atoms) and with a half (two O atoms) monolayer (ML) of oxygen between the Mo or Pt and the

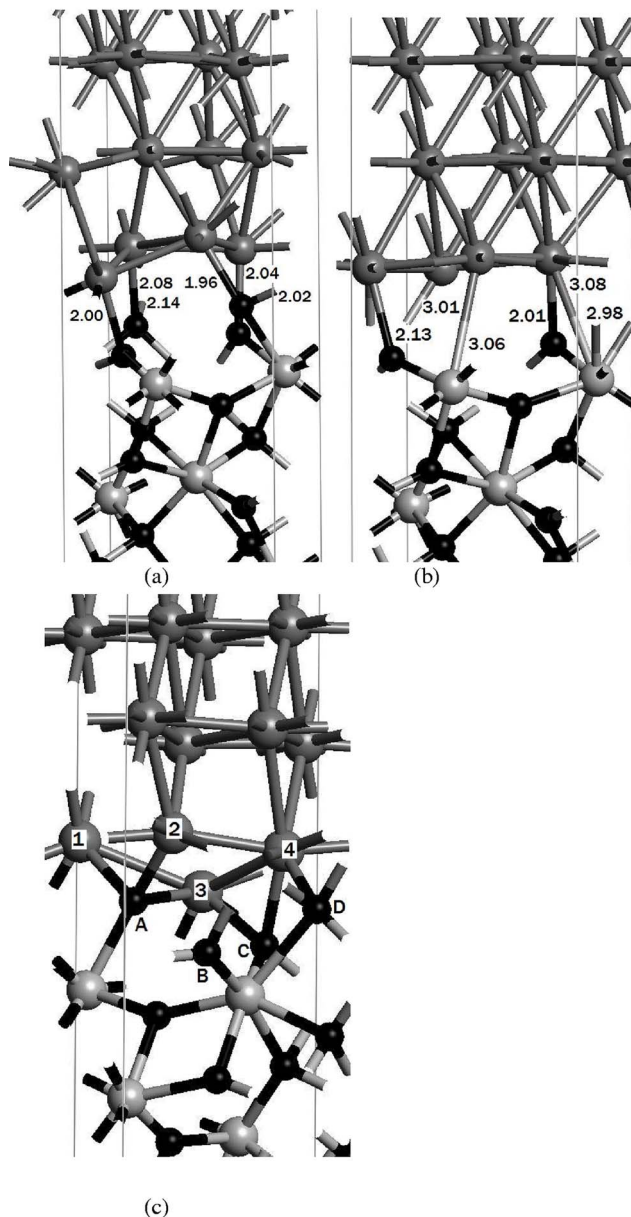
Knizhnik *et al*

FIG. 1. Model structures of (a) the most stable Pt(111)/*m*-HfO<sub>2</sub>(001) interface with a full oxygen layer, (b) the most stable Pt(111)/*m*-HfO<sub>2</sub>(001) interface with half oxygen layer, and (c) the most stable Mo(110)/*m*-HfO<sub>2</sub>(001) interface with a full oxygen layer. Light gray: Hf, black: O, and gray: Pt(Mo).

HfO<sub>2</sub> slabs (see Fig. 1). The nonstoichiometric metal/HfO<sub>2</sub> interface with additional O atoms (0.5 ML) is based on our previous study of Mo/ZrO<sub>2</sub> interfaces.<sup>25</sup> In order to find the most stable interface, we calculated several starting configurations derived by sliding the metal slabs along the oxide surface. Taking into account the periodicity of the ( $2 \times \sqrt{3}$ ) metal cell, we applied an equidistant  $2 \times 4$  grid of shift vectors with a distance of about 1.25 Å between points. For each starting configuration, the slab atoms were allowed to fully relax. This procedure led to interface configurations that differ energetically by up to 800 meV. For Pt/HfO<sub>2</sub> interfaces, we also checked the stability of the optimized interface structure by running first-principles molecular dynamics

TABLE I. Calculated work function (WF) (eV) and surface energy  $\sigma$  (J/m<sup>2</sup>) of Mo(110), Re(0001), and Pt(111) surfaces and corresponding available experimental data.

Surface	Calc. WF	Expt. WF <sup>a</sup>	Calc. $\sigma$	Expt. $\sigma$ <sup>b</sup>	Calc. $\sigma$ <sup>b</sup>
bcc Mo (110)	4.85	4.95	2.92	2.90	3.454
hcp Re (0001)	5.34	5.2	3.19	3.60	4.214
fcc Pt(111)	6.04	5.7	1.96	2.49	2.299

<sup>a</sup>Reference 33.

<sup>b</sup>Reference 32.

for the corresponding interface structure with a reduced metal gate thickness of 3 ML of Pt on hafnia with a simulation time of  $\sim 3$  ps at a temperature of 800 K.

### III. SURFACE PROPERTIES

In order to verify our approach and to serve as a comparison for our study of segregation in the presence of interfaces, we calculated the surface properties of Mo–Re and Mo–Pt metal alloys. The calculated vacuum WFs and surface energies of the pure metals, the available experimental data, and the results of previous calculations are given in Table I. We used a high-accuracy cutoff energy for pure platinum of 234 eV in the case of ultrasoft PPs and 288 eV for the projector augmented wave (PAW) method.<sup>30</sup> However, for systems with oxygen, we had to increase the cutoff energy to 495 eV in order to obtain well-converged results. The calculated energy of the Pt(111) surface, 1.96 J/m<sup>2</sup>, is in good agreement with the result of 2.067 J/m<sup>2</sup> obtained by Feibelman<sup>31</sup> using pseudopotentials. It is seen that the Pt(111) surface has the lowest surface energy and the Re(0001) has the largest surface energy of the considered metals in accordance with experimental data and previous calculations.<sup>32</sup> Thus, segregation of Pt to the alloy surface should result in a reduction of the surface energy which is the key factor governing Pt segregation in alloys with small formation enthalpies. A similar argument can be applied to Mo in Mo–Re alloys. However, while the formation energy of the Mo–Re alloy is indeed small, the formation energy of the Pt<sub>2</sub>Mo alloy is large as was mentioned above. Thus Pt segregation in a Mo host can be governed by the alloy formation energy as well.

The segregation energy in the Mo–Re system was obtained by comparing the energy of a substitutional impurity atom in the surface layer with that of a substitutional impurity atom in the bulk of the host material. These energies were obtained from slab calculations [ $2 \times 2$  surface cell with seven layers for bcc Mo(110) and nine layers for hcp Re(0001) surfaces, respectively]. We considered both the case of a Re impurity in bcc Mo and a Mo impurity in hcp Re. The results are given in Table II and show that Mo in a Re matrix has a strong segregation trend towards the surface while Re in a Mo matrix has a weak segregation trend away from the surface.

The segregation energy of a Mo atom in a fcc Pt host was calculated using a  $2 \times 2$  surface unit cell and a seven layer slab. The calculated segregation energy (+0.95 eV) is in nice agreement with the previous result (+0.93 eV) of

TABLE II. Segregation energies in Mo–Re alloys (negative value indicates favorable segregation to the surface).

Host/impurity	Mo	Re
bcc Mo (110)		+0.04 eV +0.10 eV <sup>a</sup>
hcp Re (0001)	–0.36 eV –0.43 eV <sup>a</sup>	

<sup>a</sup>Reference 4.

Ruban *et al.*<sup>4</sup> and reflects the difference between the Mo(110) and Pt(111) surface energies indicated in Table I. However, as was mentioned above, segregation in the Mo–Pt alloy is also affected by the large negative alloy formation energy. To investigate this factor, we compared the stability of the Pt<sub>2</sub>Mo(110) surface with that of the Pt(111) surface covered by one Mo layer [1 ML Mo/Pt(111)]. On the Pt<sub>2</sub>Mo(110) surface, there is one Mo atom per two Pt atoms, so 3 ML of Pt<sub>2</sub>Mo(110) slab have the same number of Mo atoms as the 1 ML Mo/Pt(111) system. A comparison between the energies of these two systems shows that a solution of Mo from the adlayer on the Pt(111) surface into the Pt bulk with the formation of Pt<sub>2</sub>Mo alloy is preferable (energy gain is 1.16 eV/Mo atom). Thus, there is a strong thermodynamic driving force for the formation of the Pt<sub>2</sub>Mo alloy when Mo is deposited on top of the Pt surface. This driving force is mainly due to the negative enthalpy of formation of the Pt<sub>2</sub>Mo alloy (–1.15 eV/Pt<sub>2</sub>Mo) but is also driven by the energy gain of exposing the more stable Pt(111) surface. To characterize the stability of the Pt(111) and Pt<sub>2</sub>Mo(110) surfaces, we calculated the detachment energies of Pt atoms from these two surfaces. The Pt detachment energy increases from 8.41 eV for the Pt(111) surface up to 9.08 eV for the Pt<sub>2</sub>Mo(110) surface. This increase corresponds approximately to the Pt<sub>2</sub>Mo alloy formation energy (0.58 eV/Pt atom).

The calculated WF of the 1 ML Mo/Pt(111) surface is 5.48 eV, which is about 0.5 eV smaller than that of the pure Pt(111) surface and is quite close to the WF of the Pt<sub>2</sub>Mo(110) surface (5.54 eV). This result is in agreement with experimental data<sup>22</sup> for Mo layers on Pt(111) and shows that the WF reduction of Mo/Pt(111) films with respect to that of the Pt(111) is about 0.5 eV both for one Mo ML on Pt(111) and for the Pt<sub>2</sub>Mo alloy.

In order to verify that strain introduced by fitting the  $(2 \times \sqrt{3})$  metal unit cell to the experimental *m*-HfO<sub>2</sub>(001) unit cell does not introduce a significant error in the calculated segregation and formation energies, we compared these energies for relaxed and strained metal alloys (see Sec. II or strained lattice parameter values). The calculated segregation energy of a Re impurity in the strained Mo slab is +0.08 eV, which is close to the value of +0.04 eV reported above for the optimized Mo cell parameters. The calculated segregation energy of a Mo impurity in a  $(2 \times \sqrt{3})$ Pt(111) slab fitted to the *m*-HfO<sub>2</sub>(001) cell is +0.97 eV, which is close to the value of +0.95 eV reported above for the optimized Pt bulk. Since the  $(2 \times \sqrt{3})$ Pt(111) unit cell does not correspond to the  $(\sqrt{3} \times \sqrt{3})$ Pt<sub>2</sub>Mo alloy unit cell, we had to emulate the Pt<sub>2</sub>Mo alloy using a different Mo–Pt alloy consisting of one

TABLE III. Calculated (spin-polarized) adsorption energy of oxygen on the Mo(110), Re(0001), and Pt(111) surfaces with 1 ML oxygen surface coverage. Energies are relative to the calculated energy of a (spin-polarized) free oxygen atom.

Surface	bcc Mo(110)	hcp Re(0001)	fcc Pt(111)
Adsorption energy (eV)	8.78	4.92	3.54

Mo atom in each  $((2 \times \sqrt{3})$ Pt layer (Pt:Mo=3:1 or Pt<sub>3</sub>Mo). A comparison between the energy of the strained Pt slab covered by one Mo ML and the energy of the strained Pt<sub>3</sub>Mo alloy shows that the solution of Mo in Pt is 0.94 eV/Mo more preferable than the presence of Mo on the surface, which is close to the value of 1.16 eV/Mo obtained from the comparison between the relaxed Mo/Pt(111) and Pt<sub>2</sub>Mo(110) stacks reported above. Based on these results we conclude that the relatively small levels of strain introduced by fitting the  $(2 \times \sqrt{3})$  metal unit cell to the experimental *m*-HfO<sub>2</sub>(001) surface does not significantly alter the energetics of the metal alloys. Therefore, despite the strain inherent in our simplified metal/oxide interface models, we expect our calculated results to correctly reflect the thermodynamic properties of more realistic relaxed interfaces.

## IV. INTERFACE PROPERTIES

### A. Driving forces for segregation at the Metal/HfO<sub>2</sub> interface

The segregation trends at the metal/HfO<sub>2</sub> interface are determined by the relative strengths of the various chemical bonds that can form at this interface.<sup>6</sup> In order to compare bond strengths, we calculated the adsorption energies of O atoms on the Mo, Re, and Pt surfaces and the adsorption energies of Mo, Re, and Pt adatoms on the *m*-HfO<sub>2</sub>(001) O-terminated surface.

The calculated O adsorption energies on the three-coordinated valley sites of the Mo(110), Re(0001), and Pt(111) surfaces for 1 ML O coverage are given in Table III. All calculated O adsorption energies in this work are relative to the calculated energy of a (spin-polarized) free oxygen atom. It is seen that O atoms bind to Mo considerably more strongly than to Pt or Re. The affinity of Mo for O should result in enhanced Mo segregation to the oxidized alloy surface compared to Pt and Re.

The calculated adsorption energies of Mo, Re, and Pt adatoms on a fully O-covered *m*-HfO<sub>2</sub>(001) surface are given in Table IV. Mo and Re have similar adsorption ener-

TABLE IV. Calculated (spin-polarized) adsorption energy of Mo, Re, and Pt adatoms on the fully O-covered *m*-HfO<sub>2</sub>(001) surface. Energies are relative to the calculated energy of a (spin-polarized) free metal atom.

Adatom	Mo	Re	Pt
Adsorption energy (eV)	14.2	14.1	9.1

gies, while that of Pt is considerably smaller. Thus Mo atoms should have a strong tendency to segregate from the Pt–Mo alloy to an O-rich interface.

Notice that the difference in the calculated oxygen adsorption energies for these metals is larger than the difference between the Mo and Re surface energies and is larger than the Pt<sub>2</sub>Mo formation enthalpy. Thus the interface with an oxide can be expected to strongly influence the segregation energies in the metal alloy as will be shown in the next section.

## B. Segregation at the metal/HfO<sub>2</sub> interface

In order to study segregation in Mo–Re and Mo–Pt alloys on hafnia, we calculated the most stable interface structures for pure Mo and Pt metals using the ( $2 \times \sqrt{3}$ ) interface model with a full and with a half O ML. The structures of the most stable Pt(111)/*m*-HfO<sub>2</sub>(001) interfaces with the optimal shift in the interface plane (the one resulting in the lowest interface energy) are shown in Figs. 1(a) (full O layer) and 1(b) (half O layer). For the case of a full O layer at the interface, we have found that the optimal structure obtained by laterally displacing the metal face with respect to the oxide face is unstable in a subsequent molecular dynamics run, which results in the formation of a rough interfacial Pt layer. This effect is caused by the strong repulsion between the interfacial oxygen atoms. Such roughening is not seen in the case of a half O layer at the interface. The structure of the most stable Mo(110)/*m*-HfO<sub>2</sub>(001) interface with a full O layer is shown in Fig. 1(c). As in the case of Pt, a full O layer at the interface between Mo and HfO<sub>2</sub> results in a rough interface structure. However, as Fig. 1 indicates, the Pt(111)/*m*-HfO<sub>2</sub>(001) and Mo(110)/*m*-HfO<sub>2</sub>(001) interfaces with a full O layer have quite different structures. Notable characteristics of these three interfaces are as follows: The relaxed Pt(111)/*m*-HfO<sub>2</sub>(001) structure with a full O layer has six Pt–O bonds at the interface (two O atoms with single Pt–O bonds 2.00 and 2.04 Å long, and two O atoms with two Pt–O bonds with lengths of 1.96, 2.02, 2.08, and 2.14 Å). The relaxed Pt(111)/*m*-HfO<sub>2</sub>(001) structure with a half O layer has two Pt–O bonds at the interface (two O atoms with single Pt–O bonds 2.01 and 2.13 Å long) and four Pt–Hf bonds (one Hf atom has three Hf–Pt bonds 2.98, 3.01, and 3.08 Å long, and the second Hf has a single Pt–Hf bond 3.06 Å long). The relaxed Mo(110)/*m*-HfO<sub>2</sub>(001) interface has nine Mo–O bonds at the interface: one O atom [labeled B in Fig. 1(c)] with a single Mo–O bond [O(B)–Mo(3)] 2.13 Å long, one O atom (C) with two Mo–O bonds 2.16 Å [O(C)–Mo(4)] and 2.25 Å [O(C)–Mo(3)], and two O atoms (A and D) with three Mo–O bonds 2.06 Å [O(A)–Mo(1)], 2.03 Å [O(A)–Mo(2)], 2.06 Å [O(A)–Mo(3)], 2.23 Å [O(D)–Mo(1)], 2.09 Å [O(D)–Mo(3)], and 2.14 Å [O(D)–Mo(4)] long. The larger number of metal–O bonds at the Mo/*m*-HfO<sub>2</sub> interface results in a stronger adhesion of the metal and the oxide. The work of separation is given by

$$W_{\text{sep}} = (E_1^{\text{tot}} + E_2^{\text{tot}} - E_{12}^{\text{tot}})/A, \quad (1)$$

where  $E_i^{\text{tot}}$  is the total energy of slab  $i$  and  $E_{12}^{\text{tot}}$  is the total energy of the two slabs in contact through an interface of

TABLE V. Calculated segregation energies of Re at the Mo/HfO<sub>2</sub> interface for different Mo positions [see Fig. 1(c)].

Re position	1	2	3	4
Segregation energy (eV)	0.27	0.22	1.10	0.69
Coordination of Mo with O atoms	2	1	3	2
Coordination of O atoms	4, 5	4	4, 5, 3	4, 5

area  $A$ .  $W_{\text{sep}}$  is 1.70 J/m<sup>2</sup> for Pt/*m*-HfO<sub>2</sub> with a full O interface and 1.47 J/m<sup>2</sup> for Pt/*m*-HfO<sub>2</sub> with a half O interface, while it is 2.70 J/m<sup>2</sup> for Mo/*m*-HfO<sub>2</sub> with a full O interface and 2.16 J/m<sup>2</sup> for Mo/*m*-HfO<sub>2</sub> with a half O interface.

The segregation energy for the Mo–Re alloy on *m*-HfO<sub>2</sub> was calculated as the energy difference of two interface structure configurations, the first one with one Re impurity atom in the bulk Mo occupying a substitutional site and the second configuration with one Re impurity atom substituted for a Mo atom at the interface. In the Mo/HfO<sub>2</sub> interface model depicted in Fig. 1(c) there are four distinct Mo atoms at the interface, so four different values for the segregation energy were calculated and are given in Table V. The calculated segregation energies vary considerably (from +0.22 up to +1.10 eV), but all of them are significantly larger than the calculated segregation energy value of +0.08 eV obtained for a Re impurity in a strained Mo(110) matrix. Thus bonding with the oxygen atoms at the metal–oxide surface significantly increases the Re segregation energy, that is, Re segregation to the interface becomes more unfavorable, and hence the Re content at the interface should be smaller than estimated from surface calculations alone. This result is in agreement with the difference between the Mo–O and Re–O bonding energies noted previously.<sup>3</sup> The large deviation of the segregation energies in the presence of interfaces from the corresponding surface value can be attributed to differences in the local chemical environments experienced by the Mo atoms. In Table V we also show the coordination of the Mo and O atoms at the interface. These values indicate that the segregation energy increases with the coordination to interfacial O atoms.

In order to investigate segregation in Pt<sub>3</sub>Mo alloys [rather than Pt<sub>2</sub>Mo, so we can compare with the segregation results of pure Pt(111)] on hafnia as a function of O content at the interface, we compared the energies of Pt<sub>3</sub>Mo/*m*-HfO<sub>2</sub> interfaces with different numbers of Mo atoms at the interface and in the Pt bulk. The relative energies of the interfaces with full and half O layers are given in Table VI. For comparison we also report in Table VI results obtained using the GGA functional<sup>34</sup> within the PAW method.<sup>35</sup> It is seen that for a full O layer segregation of Mo to the interface (ending up with one full Mo ML at the interface) is 0.16 eV/Mo atom more preferable than the formation of the Pt<sub>3</sub>Mo alloy (with one  $\frac{1}{4}$  ML Mo at the interface) and 0.67 eV/Mo atom more stable than the interface with a pure Pt layer between the hafnia slab and the Pt–Mo alloy in the bulk, at least for a sufficiently high Mo concentration. For the case of small Mo concentrations, the surface will be Pt

TABLE VI. Calculated energies (per unit cell) of Pt–Mo/HfO<sub>2</sub> interfaces with full and half oxygen MLs and different Mo distributions. The symbol  $nI(4-n)B$  means that  $n$  Mo atoms are situated at the interface and  $(4-n)$  Mo atoms are randomly distributed in the Pt bulk.

Type	4I0B	2I2B	1I3B	0I4B
Full O layer				
$dE$ (LDA/US) (eV)	0.0	...	+0.65	+2.67
Half O layer				
$dE$ (LDA/US) (eV)	0.00	−4.07	−4.03	−4.32
$dE$ (GGA/PAW) (eV)	0.00	−4.09	−4.04	−4.62

rich since the Pt surface energy is smaller than the Mo surface energy and the alloy formation energy (mixing energy) is the same for bulk and the surface. However, a kinetically limited Pt–Mo alloy on a Pt slab can be obtained as a metastable configuration as was shown by Basset.<sup>22</sup> These results reflect the large difference in the adsorption energies of O atoms on the Pt and Mo surfaces presented in Table III. However, the formation of a second ML of pure Mo at the interface is 0.97 eV/Mo atom less favorable than the formation of a Pt–Mo alloy on top of the first pure Mo ML at the interface. This is in agreement with the negative enthalpy of mixing between Mo and Pt.

For the half O layer at the Pt<sub>3</sub>Mo/HfO<sub>2</sub> interface, the structure with a pure Pt layer at the interface is 1.08 eV/Mo atom more stable than the structure with a pure Mo layer at the interface. However, the interface configurations containing one (and three) or two (and two) Mo (and Pt) atoms at the interface have energies close to that of pure Pt indicating the likely formation of an abrupt oxide/metal alloy interface (see Table VI) as far as metal species segregation is concerned. Other processes leading to a transition region between the metal oxide and the metal alloy, such as oxidation of the metal alloy, will be considered in future work.

## V. CONCLUSIONS

Through first-principles calculations we compared the segregation of metal alloys at an interface with HfO<sub>2</sub> and with vacuum. We considered Mo–Re and Mo–Pt as typical examples of disordered and ordered alloys, respectively. The driving forces for segregation at the interface with an oxide were analyzed in terms of metal and oxygen adsorption energies. It was shown that chemical bonding at the metal/oxide interface strongly influences segregation both in Mo–Re and Mo–Pt alloys. The relatively strong bonding of Mo with interfacial oxygen atoms depletes the Re content from the Mo–Re alloy in the region near the interface. It also promotes the formation of a Mo-rich region at the PtMo<sub>x</sub>/HfO<sub>2</sub> interface, but only if the interface contains a full oxygen layer. For the stoichiometric interface containing only a half oxygen layer, the oxygen concentration is insufficient to bind a full Mo layer to the interface, resulting in the

presence of Pt in contact with the oxide. The results of this study also suggest that the impact of a HfO<sub>2</sub> interface on the segregation behavior of metal alloys can be estimated simply by calculating the adsorption energies of O atoms on the surfaces of the metals of interest.

## ACKNOWLEDGMENTS

We want to thank Jamie Schaeffer for insightful discussions. Work at Kinetic Technologies has been carried out under a contract with Freescale Semiconductor, Inc.

- <sup>1</sup>G. Bozzolo, J. Ferrante, R. D. Noebe, B. Good, F. S. Honey, and P. Abel, *Comput. Mater. Sci.* **15**, 169 (1999).
- <sup>2</sup>G. Treglia, B. Legrand, F. Ducastelle, A. Saul, C. Gallis, I. Meunier, C. Mottet, and A. Senhaji, *Comput. Mater. Sci.* **15**, 196 (1999).
- <sup>3</sup>K. Heinz and L. Hammer, *J. Phys.: Condens. Matter* **11**, 8377 (1999).
- <sup>4</sup>A. V. Ruban, H. L. Skriver, and J. K. Norskov, *Phys. Rev. B* **59**, 15990 (1999).
- <sup>5</sup>P. Modrak, *Surf. Sci. Lett.* **349**, L128 (1996).
- <sup>6</sup>E. Christoffersen, P. Stoltze, and J. K. Norskov, *Surf. Sci.* **505**, 200 (2002).
- <sup>7</sup>P. Stefanov, *Appl. Surf. Sci.* **108**, 477 (1997).
- <sup>8</sup>The International Technology Roadmap for Semiconductors, <http://public.itrs.org>
- <sup>9</sup>C. C. Hobbs *et al.*, *IEEE Trans. Electron Devices* **51**, 971 (2004); **51**, 978 (2004).
- <sup>10</sup>Y.-C. Yeo, T.-J. King, and C. Hu, *J. Appl. Phys.* **92**, 7266 (2002).
- <sup>11</sup>A. A. Knizhnik, I. M. Iskandarova, A. A. Bagatur'yants, and L. R. C. Fonseca, *J. Appl. Phys.* **97**, 64911 (2005).
- <sup>12</sup>H. L. Davis, D. M. Zehner, B. Dotsch, A. Wimmer, and K. Muller, *Bull. Am. Phys. Soc.* **36**, 705 (1991).
- <sup>13</sup>R. Doll, M. Kottcke, K. Heinz, L. Hammer, K. Muller, and D. M. Zehner, *Surf. Sci.* **307–309**, 434 (1994).
- <sup>14</sup>M. Kottcke, B. Dotsch, L. Hammer, K. Heinz, K. Muller, and D. M. Zehner, *Surf. Sci.* **376**, 319 (1997).
- <sup>15</sup>L. Hammer, M. Kottcke, M. Taubmann, S. Meyer, C. Rath, and K. Heinz, *Surf. Sci.* **431**, 220 (1999).
- <sup>16</sup>R. Hultgren, P. D. Desai, D. T. Hawkins, M. Gleiser, and K. K. Kelley, in *Selected Values of Thermodynamic Properties of Binary Alloys* (American Society for Metals, Metals Park, OH, 1973).
- <sup>17</sup>*Smithells Metal Reference Book*, 6th ed., edited by E. A. Brandes (Butterworths, London, 1983), pp. 11–358.
- <sup>18</sup>S. Ouannasser and H. Dreysse, *Surf. Sci.* **523**, 151 (2003).
- <sup>19</sup>H. Deng, W. Hu, X. Shu, and B. Zhang, *Surf. Sci.* **543**, 95 (2003).
- <sup>20</sup>R. P. Elliott, *Constitution of Binary Alloys* (McGraw Hill, New York, 1965).
- <sup>21</sup>Q. Guo and O. J. Kleppa, *J. Alloys Compd.* **321**, 169 (2001).
- <sup>22</sup>D. W. Basset, *Surf. Sci.* **325**, 121 (1995).
- <sup>23</sup>A. Eckschlagler, W. Athenstaedt, and M. Leisch, *Fresenius' J. Anal. Chem.* **361**, 672 (1998).
- <sup>24</sup>M. Ceperley and B. J. Alder, *Phys. Rev. Lett.* **45**, 566 (1980); J. P. Perdew and A. Zunger, *Phys. Rev. B* **23**, 5048 (1981).
- <sup>25</sup>P. Hohenberg and W. Kohn, *Phys. Rev.* **136**, B864 (1964); W. Kohn and L. J. Sham, *ibid.* **140**, A1133 (1965).
- <sup>26</sup>G. Kresse and J. Furthmuller, *Phys. Rev. B* **54**, 11169 (1996).
- <sup>27</sup>G. Kresse and J. Hafner, *J. Phys.: Condens. Matter* **6**, 8245 (1994).
- <sup>28</sup><http://www.webelements.com>
- <sup>29</sup>R. Ruh and P. W. R. Corfield, *J. Am. Ceram. Soc.* **53**, 126 (1970).
- <sup>30</sup>P. E. Blöchl, *Phys. Rev. B* **50**, 17953 (1994).
- <sup>31</sup>P. J. Feibelman, *Phys. Rev. B* **52**, 16845 (1995).
- <sup>32</sup>L. Vitos, A. V. Ruban, H. L. Skriver, and J. Kollar, *Surf. Sci.* **411**, 186 (1998).
- <sup>33</sup>H. Michaelson, *J. Appl. Phys.* **48**, 4729 (1977).
- <sup>34</sup>J. P. Perdew, K. Burke, and M. Ernzerhof, *Phys. Rev. Lett.* **77**, 3865 (1996).
- <sup>35</sup>G. Kresse and D. Joibert, *Phys. Rev. B* **59**, 1758 (1999).